SCIENTIFIC REPORTS

OPEN

Genetically engineered biosynthetic pathways for nonnatural C_{60} carotenoids using C_5-elongases and C_{50}-cyclases in *Escherichia coli*

Received: 22 November 2018
Accepted: 22 January 2019
Published online: 27 February 2019

Ling Li[1], Maiko Furubayashi[1], Shifei Wang[1], Takashi Maoka[2], Shigeko Kawai-Noma[1], Kyoichi Saito[1] & Daisuke Umeno[1]

While the majority of the natural carotenoid pigments are based on 40-carbon (C_{40}) skeleton, some carotenoids from bacteria have larger C_{50} skeleton, biosynthesized by attaching two isoprene units (C_5) to both sides of the C_{40} carotenoid pigment lycopene. Subsequent cyclization reactions result in the production of C_{50} carotenoids with diverse and unique skeletal structures. To produce even larger nonnatural novel carotenoids with $C_{50}+C_5+C_5=C_{60}$ skeletons, we systematically coexpressed natural C_{50} carotenoid biosynthetic enzymes (lycopene C_5-elongases and C_{50}-cyclases) from various bacterial sources together with the laboratory-engineered nonnatural C_{50}-lycopene pathway in *Escherichia coli*. Among the tested enzymes, the elongases and cyclases from *Micrococcus luteus* exhibited significant activity toward C_{50}-lycopene, and yielded the novel carotenoids C_{60}-flavuxanthin and C_{60}-sarcinaxanthin. Moreover, coexpression of *M. luteus* elongase with *Corynebacterium* cyclase resulted in the production of C_{60}-sarcinaxanthin, C_{60}-sarprenoxanthin, and C_{60}-decaprenoxanthin.

Carotenoids are a class of natural pigments covering yellow, orange and red colors. More than 750 carotenoids have been identified in various plants, fungi, and microorganisms[1], and a wide range of essential biological functions have been described, with light-harvesting, photoprotection, antioxidatant, and pro-vitamin activities, and roles in the control of membrane fluidity[2]. In recent years, carotenoids have been increasingly considered in applications as therapeutic or bioelectronic materials[3,4]. Small changes in carotenoid structures have been associated with large differences in material properties[5] and biological activities[3,6]. Hence, the discovery of the structurally novel carotenoids is eagerly awaited.

Most carotenoids have C_{40} backbones, although a few microbial carotenoids have C_{30} backbones. The structural diversity of carotenoids is mainly derived from differences in desaturation levels of the C_{40} backbone, types of end groups, and functional patterns of cyclization, oxidation, and esterification. Further structural diversity of carotenoids can be achieved by liberating carotenoids from their C_{40} backbones. For example, carotenoid cleavage enzymes can be used to produce a range of carotenoids with different-backbone sizes (C_{14}, C_{20}, or C_{28} carbons)[7]. These include precursors of bixin (C_{24+1}), crocetin (C_{20}), retinals (C_{20}), and other hormonal compounds such as strigolactones (C_{13}) and abscisic acid (C_{15}), as reviewed previously[3].

Another source of structure and size diversity comes from the attachment of additional isoprene units (C_5) to C_{40} carotenoids. Since C_{45} and C_{50} carotenoids were first reported in the 1960s[8,9], many of these carotenoids have been identified in prokaryotes, including gram-positive bacteria such as *Micrococcus*[10], *Corynebacterium*[11], *Dietzia*[12], and extreme halophilic archaea such as *Halobacterium* or *Haloarcula*[13]. Although the natural functions of these carotenoids are not fully understood, contributions to cell membrane fluidity and permeability have been suggested[13]. In addition, the attachment of C_5 units reportedly confers remarkable antioxidant activities to carotenoids[14], and the resulting compounds have been considered for their potential as therapeutic agents[13–15].

[1]Department of Applied Chemistry and Biotechnology, Chiba University, Chiba, Japan. [2]Research Institute for Production Development, Kyoto, Japan. Ling Li and Maiko Furubayashi contributed equally. Correspondence and requests for materials should be addressed to D.U. (email: umeno@faculty.chiba-u.jp)

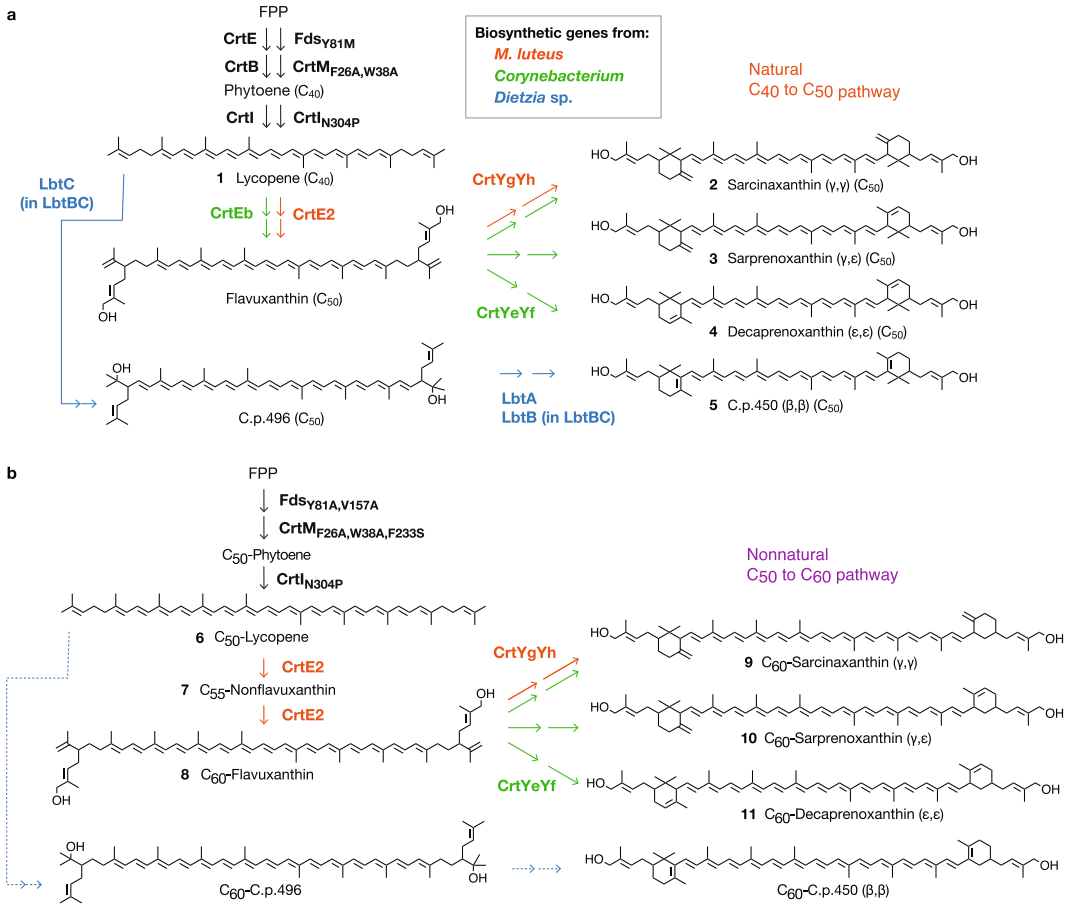

Figure 1. C_5-elongation and cyclization pathways for natural (C_{50}) and nonnatural (C_{60}) carotenoids. (**a**) Natural C_{40}-to-C_{50} carotenoid pathway. Using lycopene (C_{40}) as a substrate, the lycopene elongases CrtEb from *Corynebacterium* and CrtE2 from *M. luteus* attaches two isoprene units to C_{40}. The resulting flavuxanthin (C_{50}) is then cyclized by the γ- and/or ε-cyclases CrtYe/Yf (*Corynebacterium*) or CrtYg/Yh (*M. luteus*) to produce sarcinaxanthin, sarprenoxanthin, or decaprenoxanthin (all C_{50}). LbtABC genes from *Dietzia* sp. CQ4 produces the β,β-cyclic C_{50} carotenoid C.p.450 via the independent intermediate C.p.496. (**b**) Nonnatural C_{50}-to-C_{60} carotenoid pathway construction. Combined expression of *Corynebacterium* and *M. luteus* elongases and cyclases resulted in the conversion of laboratory-generated C_{50}-lycopene to C_{60} carotenoids with γ and/or ε-cyclic ends. We could not obtain C_{60} counterparts of β-end C_{50} carotenoids (indicated in arrows with dashed lines).

To date, four natural biosynthetic pathways for C_{50} carotenoids has been reported[10–12,16]. All known C_{50} carotenoids are derived from lycopene, a four-step enzymatic desaturation product of phytoene, which is produced by the condensation of two molecules of geranylgeranyl diphosphate (C_{20}). One pathway from extremely halophillic archaea *Haloarcula japonica* yields acyclic C_{50} carotenoid bacterioruberin[16] as the final product, whereas three others produce cyclic C_{50} carotenoids (Fig. 1a). In the *Micrococcus luteus* carotenoid biosynthetic pathway, lycopene elongase (CrtE2) attaches two additional isoprene units (DMAPP) to the 2,2′-position of lycopene to produce the acyclic C_{50} carotenoid flavuxanthin, and subsequent γ-cyclization by cyclase (CrtYgYh) produces sarcinaxanthin (γ,γ-ring)[10]. C_{50} carotenoid synthesis in *Corynebacterium* also proceeds via the flavuxanthin intermediate, but the expressed cyclase (CrtYeYf) is less specific and yields a mixture of decaprenoxanthin[10,11] (ε,ε-ring), sarprenoxanthin[10] (ε,γ-ring) and sarcinaxanthin, when expressed in *E. coli*. In contrast, the bacterium *Dietzia*, reportedly produces C_{50} carotenoids with β,β-rings (C.p.450)[12] via a different acyclic intermediate (Fig. 1a).

In a previous study, we constructed a nonnatural C_{50} backbone carotenoid pathway in which two geranylfarnesyl diphosphates (C_{25}PP) are condensed to produce C_{50}-phytoene (Fig. 1b). This compound is subsequently subjected to a six-step desaturation reaction resulting in the synthesis of C_{50}-lycopene. Using a metabolic filtering approach[17], we extended this C_{50}-lycopene pathway to specifically produce the nonnatural C_{50} backbone carotenoids C_{50}-β-carotene, C_{50}-zeaxanthin, C_{50}-canthaxanthin, and C_{50}-astaxanthin. In this study, we systematically expressed elongase and cyclase in engineered *E. coli* strains harboring enzymes of the C_{50}-lycopene synthetic pathway and established pathways for the synthesis of the novel carotenoids C_{60}-flavuxanthin, C_{60}-sarcinaxanthin, C_{60}-sarprenoxanthin, and C_{60}-decaprenoxanthin (Fig. 1b).

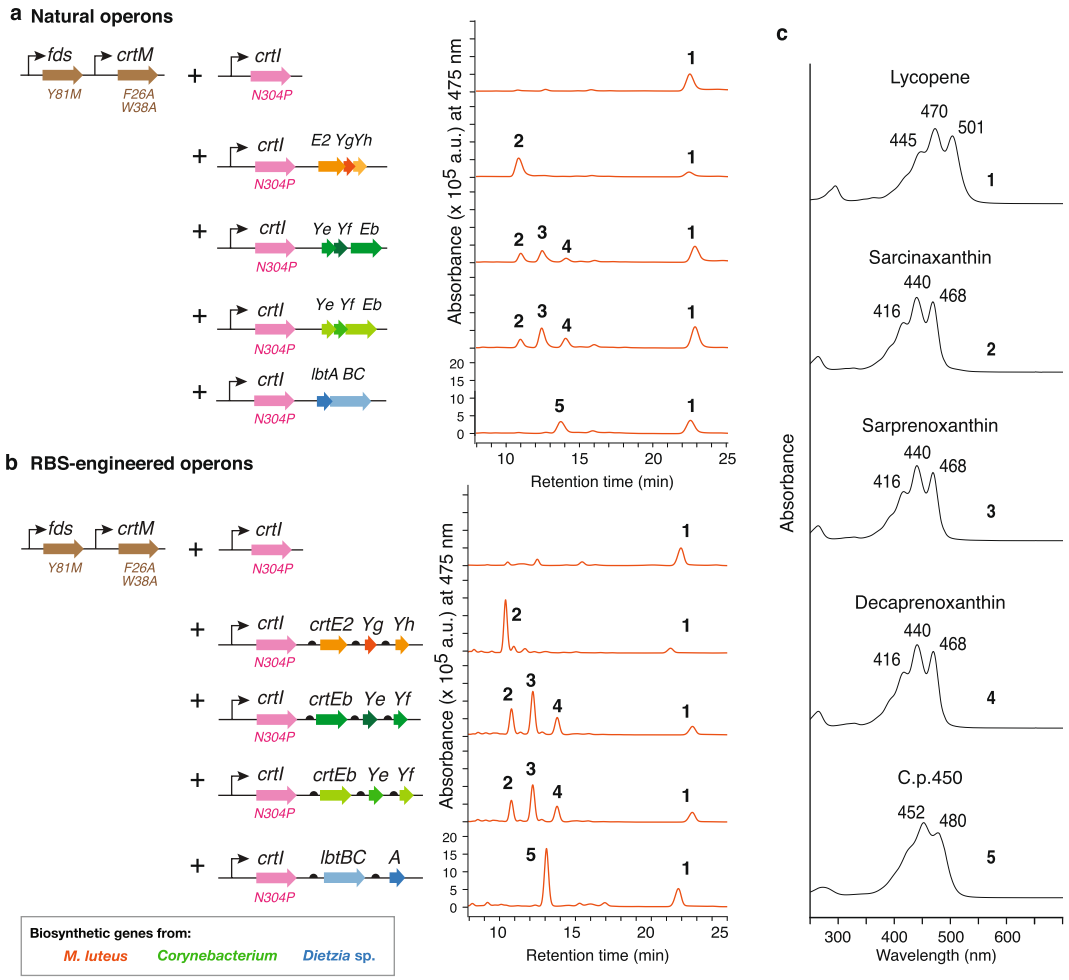

Figure 2. Lycopene elongases and C_{50} cyclases function in the natural C_{40}-to-C_{50} pathway. HPLC chromatograms of carotenoid extracts from *E. coli* cells harboring plasmids with genome-derived natural gene cluster (**a**) or RBS-redesigned artificial operons (**b**), together with lycopene biosynthetic genes. Peak numbers correspond with those indicated in c and Fig. 1. (**c**) Absorbance spectra of indicated compounds.

Results

Activities of elongase and cyclase in the natural C_{40} pathway. We selected *Corynebacterium glutamicum*, *M. luteus*, and *Dietzia* sp. CQ4 as sources of lycopene elongases and C_{50} cyclases, because the C_{50} carotenoid pathways from these organisms have been previously reconstructed in *E. coli*[10–12]. The carotenoid cluster (shown in Supplementary Fig. 1) of *C. glutamicum*[11] comprises *crtEb* (lycopene elongase), *crtYeYf* (heterodimeric C_{50} ε/γ-cyclase), and lycopene-producing genes (*crtEBI*). The expression of this gene cluster in *E. coli* produces sarprenoxanthin, decaprenoxanthin, and sarcinaxanthin via the acyclic intermediate flavuxanthin[10,11] (Fig. 1a). The corresponding gene cluster in *M. luteus*[10] encodes *crtE2* (lycopene elongase) and *crtYgYh* (C_{50} γ-cyclase), and coexpression of these genes with *crtEBI* results in specific accumulation of sarcinaxanthin[10]. Uniquely, the carotenogenic gene cluster of *Dietzia sp.* CQ4[12] encodes a gene for elongase (*lbtC*) that is fused in frame with a single subunit of cyclase (*lbtB*), which forms a heterodimer with another unit of cyclase (*lbtA*). Expression of *lbtB* with an *lbtA* gene product results in the production of a functional C_{50} β-cyclase[12].

Although different in organization, all of the elongase and cyclase genes are clustered in small <1.7-kb regions (Supplementary Fig. 1), allowing one-step PCR amplification from genomic DNA. We cloned these DNA fragments into a plasmid that encodes *Pantoea ananatis* phytoene desaturase variant[17] $crtI_{N304P}$, a variant that can desaturate both (C_{40}-) phytoene and C_{50}-phytoene (see Fig. 2a for plasmid construct). In addition to these three operons (for *C. glutamicum*, *M. luteus* and *Dietzia* sp.), we cloned the elongase and cyclase genes from *Corynebacterium efficiens*. The carotenoid gene cluster of this organism has exactly the same organization as that of *C. glutamicum*, and in our homology analyses, DNA sequence identity of the two clusters (from *crtE* to *crtEb*, see Supplementary Fig. 1) was 64.3%. Yet, the functions of the *C. efficiens* carotenoid pathway and its products remain uncharacterized.

To characterize the functions of elongase and cyclase in the context of natural (C_{40}) pathway (Fig. 1a) in *E. coli*, we used an engineered *E. coli* strain that constitutively expresses fds_{Y81M} and $crtM_{F26A,W38A}$ genes (*crtEB* equivalent[17]) and produces phytoene (C_{40}). We introduced plasmids encoding phytoene desaturase (a *crtI* variant), elongases and cyclases into this strain, and after culturing for 48 h, we extracted carotenoids using acetone and

Organism	Gene	RBS strength in v1 plasmid	Designed RBS strength in v2 plasmid
M. luteus	*crtE2*	812	4296
	crtYg	0.01	1525
	crtYh	140	4700
Dietzia sp. CQ4	*lbtA*	968	4106
	lbtBC	15	4700
C. glutamicum	*crtYe*	4493	3891
	crtYf	4342	5886
	crtEb	389	5066
C. efficiens	*crtYe*	776	1113
	crtYf	33	2663
	crtEb	93	1990

Table 1. Ribosome binding site strengths of original and designed operons. RBS strength obtained using a ribosome binding site (RBS) calculator[18–20]. The RBS and open reading frame (ORF) sequences are listed in Supplementary Tables S1 and S2.

analyzed these using high performance liquid chromatography (HPLC) (Fig. 2a). These analyses showed that cells expressing *C. glutamicum crtYeYfEb* produced a mixture of (C_{50}-) sarcinaxanthin (**2**), (C_{50}-) sarprenoxanthin (**3**), and (C_{50}-) decaprenoxanthin (**4**), with significant quantities of their substrate (C_{40}-) lycopene (**1**). Cells expressing *C. efficiens crtYeYfEb* indistinguishable composition of carotenoids as those from the *C. glutamicum* gene cluster. Cells expressing *M. luteus crtE2YgYh* produced a single peak of (C_{50}-) sarcinaxanthin (**2**), whereas expression of *Dietzia* sp. CQ4 *lbtABC* resulted in the specific production of C.p.450 (C_{50}). Despite the differences in the source of lycopene biosynthetic genes, promoters, RBS sequences, *E. coli* strain or culture condition, product distribution of the pathway we constructed was very similar to those from previous reports[10].

To determine whether these enzymes can metabolize C_{50}-lycopene, we coexpressed plasmids encoding the elongase and cyclase enzymes in another *E. coli* strain that constitutively expresses $fds_{Y81A,V157A}$ and $crtM_{F26A,W38A,F233S}$ and produces C_{50}-phytoene[17]. In this strain, the phytoene desaturase mutant ($CrtI_{N304P}$) can desaturate C_{50}-phytoene to produce C_{50}-lycopene selectively[17], providing a sole substrate for the elongase and cyclases in this stain. However, we observed no novel peaks but C_{50}-lycopene in carotenoid fractions from this strain.

Ribosome binding site (RBS)-optimized cyclase/elongase results in higher production of cyclic C_{50} carotenoids. In the previous section, we observed (C_{40}-) lycopene accumulated in cells expressing elongase and cyclases (Fig. 2a), suggesting the presence of inefficiencies of this pathway, and room for improvement. The present four carotenoid operon constructs share similar operon organization, in which open reading frames (ORF) for cyclases and elongases are partially overlapping. Specifically, the start codon of *M. luteus crtYg* is 28 base pairs upstream of the stop codon of the *crtE2* gene, and the start codon of *crtYh* overlaps with the stop codon of the *crtYg* gene. In *C. glutamicum* and *C. efficiens*, *crtYe* and *crtYf* overlap by 4 bases, and in *Dietzia*, *lbtA* and *lbtBC* genes also overlap by 4 bases, as is commonly observed in various gene clusters containing carotenoid operons[10]. We investigated translation initiation rates using the RBS calculator[18–20] and found RBS scores as low as 0.01 (Table 1), suggesting very low translation initiation rates and likely formation of stable secondary mRNA structures. In the native operons with overlaps in translational stop and start of ORFs, the translational re-initiation is likely ensuring efficient translation *in vivo*.

To improve expression levels of elongases and cyclases in *E. coli*, we redesigned our artificial operons (Fig. 2b) by (1) separating the ORFs to yield tandem and distinct non-overlapping reading frames, and (2) to provide stronger RBSs, designed using RBS calculator to have RBS strengths between 1,000 - 5,000 (Table 1). These RBS strengths range were chosen since it was previously confirmed optimal for expressing various carotenoid biosynthetic genes in the plasmid backbone we use in this study[17,21] (i.e. p15A, pUC). When expressed with (C_{40}-) lycopene pathways, all of these new constructs with engineered RBSs led to improved production of natural C_{50} carotenoids and significant reductions in unconverted lycopene contents (Fig. 2b).

Production of nonnatural cyclic C_{60} carotenoids. Following the RBS engineering of elongases and cyclases, we cotransformed the new constructs into the strains that selectively synthesize C_{50}-phytoene (Fig. 3). From the cells expressing *M. luteus crtE2YgYh*, we observed novel peaks **7** and **9** in HPLC chromatograms, and these were eluted earlier than that of C_{50}-lycopene (**6**) (Fig. 3a,b). Peak **9** exhibited absorbance maxima at 496 nm; shorter than that for C_{50}-lycopene (**9**, 512 nm). The m/z value (837) of peak **9** matched that of C_{60}-sarcinaxanthin ($C_{60}H_{84}O_2$, Fig. 1), and the carotenoid from peak **9** had absorption maxima at 460, 494, and 527 nm (Fig. 3h). Furthermore, analyses using positive ion electrospray ionization time-of-flight mass spectrometry (ESI TOF MS) at *m/z* 837.6542 MH^+ indicated a molecular formula for this carotenoid of $C_{60}H_{84}O_2$ ($C_{60}H_{85}O_2$ calcd. for 837.6550) (Supplementary Fig. 2). The structure of this carotenoid was determined as C_{60}-sarciniaxanthin using nuclear magnetic resonance (^{1}H-NMR) with correlation spectroscopy (COSY) and rotating frame overhause effect spectroscopy (ROESY) (Table 2). In addition, we identified peak **7** as the C_{60} pathway intermediate C_{55}-nonflavuxanthin based on an absorbance maximum of 513 nm and a m/z value of 753 ($C_{55}H_{76}O$).

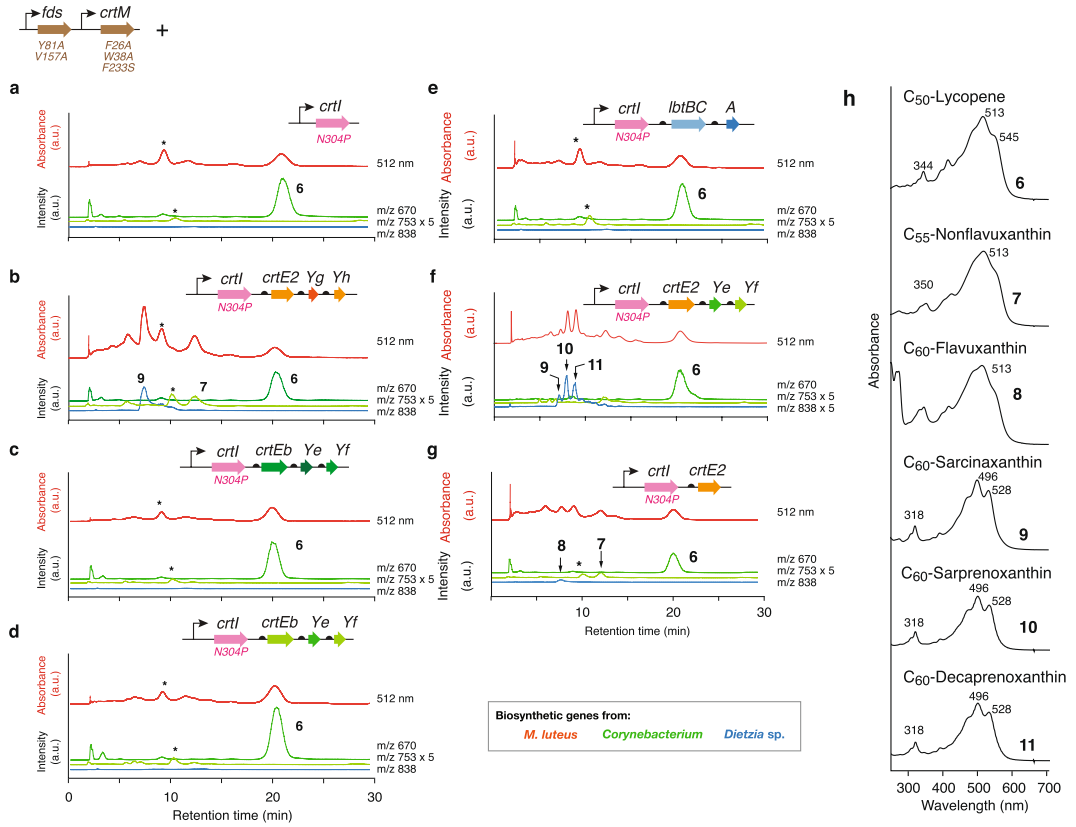

Figure 3. Lycopene elongases and C_{50} cyclases function in the C_{50}-to-C_{60} pathway. (**a**–**g**) HPLC chromatogram of carotenoid extracts from *E. coli* cells expressing genes for C_{50}-phytoene production with indicated genes. The indicated peak numbers correspond with those in Fig. 1. Peaks labelled with asterisks correspond to unidentified non-carotenoid compounds. (**h**) Absorbance spectra of the indicated peaks.

The *crtE2* gene expression (without *crtYgYh*) from *M. luteus* resulted in a new peak **8** with an m/z value of 838 and an absorbance maximum of 513 nm (Fig. 3g). The carotenoid from peak **8** showed absorption maxima at 460, 494, and 527 nm (Fig. 3h). Positive ion ESI TOF MS at *m/z* 857.6107 M + Na^+ revealed the molecular formula $C_{60}H_{82}O_2$ ($C_{60}H_{82}O_2Na$ calcd. for 857.6212) (Supplementary Fig. 3) for this carotenoid, and structural analyses using ^{1}H-NMR with COSY and ROESY revealed the carotenoid C_{60}-flavuxanthin (Table 2).

We did not observe any novel carotenoid peaks in experiments using elongase and cyclase genes from *C. glutamicum*, *C. efficiens*, or *Dietzia* sp. CQ4 (Fig. 3c–e). Hence, the lycopene elongases (CrtEb in *Corynebacterium* and LbtC in *Dietzia* sp. CQ4) at least fail to convert C_{50}-lycopene in *E. coli*. However, the activities of the cyclases (CrtYeYf from *Corynebacterium* and LbtAB from *Dietzia* sp. CQ4) were still unknown, since the first elongase step failed to provide the substrate (C_{60}-flavuxanthin or C_{60}-C.p.496) for these cyclase enzymes.

Because *Corynebacterium* and *M. luteus* pathways share the intermediate flavuxanthin, we generated a chimera operon containing *M. luteus crtE2* and *C. efficiens crtYeYf*. Following expression in cells, we detected three carotenoid peaks (Fig. 3f) (**9**, **10**, and **11**) with identical absorption spectra (Fig. 3h), indicating the presence of the same chromophore. Although we could not determine the NMR spectroscopy of the compound from the associated chromatographic peaks, their absorption spectra, m/z values (838) and retention times strongly indicate that peaks **9**, **10**, and **11** were C_{60}-sarcinaxanthin (as shown in Fig. 3b), C_{60}-sarprenoxanthin, and C_{60}-decaprenoxanthin, respectively. These results also indicate that cyclases (*crtYeYf)* from *Corynebacterium* are functional in the C_{50}-to-C_{60} pathway.

Discussion

In this study, we demonstrated that carotenoid elongation and cyclization enzymes from natural C_{50} carotenoid pathways metabolize C_{50}-lycopene to novel nonnatural C_{60} carotenoids. These carotenoids (C_{60}-flavuxanthin, C_{60}-sarcinaxanthin, C_{60}-sarprenoxanthin, and C_{60}-decaprenoxanthin) are larger than any known natural carotenoids, and their absorbance spectra are red-shifted by as much as 58 nm compared with the natural counterpart (440 nm vs. 496 nm). With rare γ-ring structures, these C_{60} carotenoids provide a unique set of accessible carotenoid structures with as yet unknown functions. Natural C_{50} carotenoids were previously discovered in thicker membranes of halophillic bacteria, which survive in extreme hypersaline and low-temperature environments[13,14,16]. The present nonnatural C_{60} carotenoids are interesting candidates for functional characterization in extremophiles. These future studies may lend understanding to the roles of long-chain carotenoids in nature.

Through the coexpression of natural carotenoid enzymes, we have increased the number of laboratory-generated C_{50} carotenoid pathways. Many carotenoid enzymes from C_{40} and C_{30} pathways exhibit

Position	C_{60}-Sarcinaxanthin (9)			Position	C_{60}-Flavuxanthin (8)		
	d	Mult.	J (Hz)		d	Mult.	J (Hz)
H-2 (2′)	1.28	m		H-2 (2′)	2.08	m	
H-3 (3′)	1.18	m		H_2-3 (3′)	1.56	m	
	1.71	m					
H-4 (4′)	2.05	m		H_2-4 (4′)	2.00	m	
	2.35	m					
H-6 (6′)	2.48	d	10	H-6 (6′)	5.93	d	11
H-7 (7′)	5.83	d	15.5, 10	H-7 (7′)	6.48	dd	15, 11
H-8 (8′)	6.12	d	15.5	H-8 (8′)	6.24	d	15
H-10 (10′)	6.12	d	12	H-10 (10′)	6.18	d	12
H-11 (11′)	6.62	dd	15, 12	H-11 (11′)	6.63	dd	15, 12
H-12 (12′)	6.34	d	15	H-12 (12′)	6.36	d	15
H-14 (14′)	6.23	d	11	H-14 (14′)	6.23	d	11
H-15 (15′)	6.64	dd	15, 11	H-15 (15′)	6.64	dd	15, 11
H-16 (16′)	6.38	d	15	H-16 (16′)	6.38	d	15
H-18 (18′)	6.27	br. d	10	H-18 (18′)	6.27	br. d	10
H-19 (19′)	6.64	m		H-19 (19′)	6.64	m	
H_3-20 (20′)	0.96	s		H-20 (20′)	4.70	br. S	
				H-20 (20′)	4.78	br. S	
H_3-21 (21′)	0.73	s		H_3-21 (21′)	1.63	s	
H-22 (22′)	4.53	s		H_3-22 (22′)	1.80	s	
H-22 (22′)	4.76	s					
H_3-23 (23′)	1.98/1.99	s		H_3-23 (23′)	1.97	s	
H_3-24 (24′)	1.98/1.99	s		H_3-24 (24′)	1.98/1.99	s	
H_3-25 (25′)	1.98/1.97	s		H_3-25 (25′)	1.98/1.97	s	
H-26 (26′)	1.72	m					
H-26 (26′)	2.24	dd	14, 5.5	H_2-26 (26′)	2.10	m	
H-27 (27′)	5.43	m		H-27 (27′)	5.36	t	5
H_3-29 (29′)	1.67	s		H_3-29 (29′)	1.67	s	
H_2-30 (30′)	4.03	s		H_2-30 (30′)	4.00	s	

Table 2. ^{1}H NMR data for C_{60}-sarcinaxanthin and C_{60}-flavuxanthin in $CDCl_3$. See Supplementary Fig. S4 for the numbering of carotenoid structure.

significant substrate promiscuity and accept a wide range of substrates with recognizable locally specific[22] structures. Consequently, these enzymes are active in nonnatural pathway contexts[22–25] without any mutations. However, there is increasing reports on carotenoid modifying enzymes that exhibit unexpected selectivity against non-cognate but very similar substrates. For example, lycopene ε-cyclases from plants (LCYe) cyclize only one end of the acyclic substrate lycopene and leave the other end un-cyclized[26]. Hence, ε-cyclases likely possess mechanisms for avoiding cyclization of non-cognate substrates. Similarly, the β-carotene 15,15′ cleavage enzyme BCMO1 only accepts β-carotene (β,β-end) as a substrate and does not act on ε-carotene (ε,ε-end). However, after removing the ε-end via 9′,10′ cleavage by BCMO2, BCMO1 precisely cleaves the 15,15′ bond and liberates retinal[27].

While the elongases from *Corynebacterium* and *Dietzia* sp. CQ4 exhibited a significant activity towards natural substrate (C_{40}-lycopene), they did not show any activity towards C_{50}-lycopene. Considering that enzymes from both strains have significant activity in the C_{40}-to-C_{50} context, it is unlikely that their inability to act on C_{50}-lycopene reflects a lack of activity in *E. coli*. The more likely alternative is that some of these enzymes have higher substrate/size specificity and resist C_{50}-lycopene as a substrate. Kim *et al.* showed that the *Corynebacterium* elongase CrtEb is functional in another non-cognate context and acts on the ψ-end of the C_{30} carotenoid 4,4′-diaponeurosporene[25]. Given this unpredictability of promiscuous functions toward non-cognate substrates, studies of several accessible gene candidates are required to identify genes that perform intended non-natural tasks. Also, it is interesting how or whether *Dietzia* elongase and cyclase and *Corynebacterium* elongase, which were found non-functional in C_{50}-to-C_{60} context in the present work, can acquire these new activities by mutations.

Methods

Strains and reagents. *E. coli* XL10-Gold cells were used for cloning, and XL1-Blue cells were used for carotenoid production. All enzymes were purchased from New England Biolabs. Lennox-LB Broth Base was purchased from Life Technologies, Bacto™ Yeast Extract, and Bacto™ Tryptone were purchased from BD Biosciences, and all other chemicals and reagents were obtained from Nacalai Tesque (Kyoto, Japan). The antibiotics carbenicillin and chloramphenicol were used at 30 and 50 μg/mL, respectively.

Plasmid construction. pUCara-crtI$_{N304P}$, a plasmid encoding a *crtI$_{N304P}$* gene downstream of an arabionse inducible *araBAD* promoter, was derived from a previous study[17]. The plasmids pUCara-crtI$_{N304P}$-crtYeYfEb$_{Cg}$, pUCara-crtI$_{N304P}$-crtYeYfEb$_{Ce}$, pUCara-crtI$_{N304P}$-crtE2YgYh$_{Ml}$, and pUCara-crtI$_{N304P}$-lbtABC$_{CQ4}$ were constructed by amplifying genes for elongase and cyclase from various genomes using the primers listed in Supplementary Table 1 and cloning these into the ApaI/SpeI restriction site of pUCara-crtI$_{N304P}$. The plasmids pAC-fds$_{Y81A,V157A}$-crtM$_{F26A,W38A,F233S}$ and pAC-fds$_{Y81M}$-crtM$_{F26A,W38A}$ were derived from the previous study[17]. The *fds* and *crtM* variant genes on these plasmids were expressed constitutively under *lac* promoter. Supplementary Table 2 shows the DNA sequence of the designed RBS construct. These sequences were concatenated and were then inserted into the ApaI/SpeI restriction site of pUCara-crtI$_{N304P}$ without spacer sequences.

Culture conditions. Single colonies were inoculated into 2 ml of LB media with antibiotics in culture tubes and were shaken at 37 °C for 16 h. Overnight cultures of 2 mL were diluted 100-fold into 40 mL of fresh Terrific Broth media in 200 mL flasks and were then shaken at 200 rpm in an incubator at 30 °C. After 8 h, 0.2% (w/v) arabinose inducer was added and cells were cultured for an additional 40 h.

Product extraction and purification. Cell cultures were centrifuged at 3,270 × *g* for 15 min at 4 °C. Cell pellets were washed with 10 ml of 0.9% (w/v) NaCl$_{aq}$ and were then repelleted by centrifugation. Products were extracted by vigorously vortexing for 5 min in 10 ml of acetone containing 30-mg/L butylated hydroxytoluene. One-mL aliquots of hexane and 35-ml aliquots of 1% (w/v) NaCl$_{aq}$ were then added, and the samples were centrifuged at 3,250 × *g* for 15 min. After collecting the product-containing hexane phase, the solvent was evaporated in a vacuum concentrator. Extracts were finally dissolved in 15–50-μl aliquots of tetrahydrofuran:methanol (6:4) for further analysis.

HPLC–MS analysis for compound identification and quantification. Aliquots (2–15 μL) of final extracts were analyzed using Shimadzu Prominence HPLC system equipped with LCMS-2020 MS spectrometer, a photodiode array (PDA) detector with Waters Spherisorb ODS2 Analytical Columns (4.6 × 250 mm, 5 μm, PSS831915). Mobile phases comprised acetonitrile/tetrahydrofuran/methanol (58:7:35) at a flow rate of 2 mL/min (Fig. 2a), acetonitrile/tetrahydrofuran/methanol (58:4:38) at a flow rate of 1 mL/min (Fig. 2b), and acetonitrile/tetrahydrofuran/methanol (30:7:63) at a flow rate of 1.5 mL/min (Fig. 3). Elutes were detected using PDA (200–700 nm) and APCI-MS. Mass scans were performed from *m/z* 10 to *m/z* 1000 with a 300 °C interface temperature, a 300 °C DL, a ± 4500-V interface voltage, and a neutral DL/Qarray with N_2 as the nebulizing gas.

ESI TOF MS spectra were acquired using a Waters Xevo G2S Q TOF mass spectrometer (Waters Corporation, Milford, CT, USA) equipped with an Acquity UPLC system with scanning from *m/z* 100 to 1,500 with a capillary voltage of 3.2 kV, a cone voltage of 40 eV, and a source temperature of 120 °C. Nitrogen was used as the nebulizing gas at a flow rate of 30 L/h. MS/MS spectra were measured using a quadrupole-TOF MS/MS instrument with argon as a collision gas at a collision energy of 30 V. ^{1}H NMR (500 MHz) including COSY and ROESY spectra were generated using a Varian UNITY INOVA 500 spectrometer in $CDCl_3$ with tetramethylsilane as an internal standard.

Data Availability

The datasets generated during and/or analysed during the current study are available from the corresponding author on reasonable request.

References

1. Mercadante, A., Egeland, E., Britton, G., Liaaen-Jensen, S. & Pfander, H. Carotenoids handbook. (eds Britton, G., Liaaen-Jensen, S., Pfander, H.) (Birkhäuser Basel, 2004).
2. Britton, G. Functions of intact carotenoids in *Carotenoids* (eds Britton G., Liaaen-Jensen S., Pfander H.) 189–212 (Birkhäuser Basel, 2008).
3. Alvarez, R., Vaz, B., Gronemeyer, H. & de Lera, A. R. Functions, therapeutic applications, and synthesis of retinoids and carotenoids. *Chem. Rev.* **114**, 1–125, https://doi.org/10.1021/cr400126u (2014).
4. Irimia-Vladu, M., Sariciftci, N. S. & Bauer, S. Exotic materials for bio-organic electronics. *J. Mater. Chem.* **21**, 1350–1361, https://doi.org/10.1039/c0jm02444a (2011).
5. Hashimoto, H., Uragami, C., Yukihira, N., Gardiner, A. T. & Cogdell, R. J. Understanding/unravelling carotenoid excited singlet states. *J. R. Soc. Interface* **15**, https://doi.org/10.1098/rsif.2018.0026 (2018).
6. Albrecht, M., Takaichi, S., Steiger, S., Wang, Z. Y. & Sandmann, G. Novel hydroxycarotenoids with improved antioxidative properties produced by gene combination in *Escherichia coli*. *Nat. Biotechnol.* **18**, 843–846, https://doi.org/10.1038/78443 (2000).
7. Walter, M. H. & Strack, D. Carotenoids and their cleavage products: Biosynthesis and functions. *Nat. Prod. Rep.* **28**, 663–692, https://doi.org/10.1039/c0np00036a (2011).
8. Liaaen-Jensen, S., Hertzberg, S., Weeks, O. B. & Schwieter, U. Bacterial carotenoids XXVII. C50-carotenoids. 3. Structure determination of dehydrogenans-P439. *Acta Chem. Scand. [A]*. **22**, 1171–1186 (1968).
9. Weeks, O. B., Andrewes, A. G., Brown, B. O. & Weedon, B. C. Occurrence of C_{40} and C_{45} carotenoids in the C_{50} carotenoid system of *Flavobacterium dehydrogenans*. *Nature* **224**, 879–882 (1969).
10. Netzer, R. *et al.* Biosynthetic pathway for gamma-cyclic sarcinaxanthin in *Micrococcus luteus*: heterologous expression and evidence for diverse and multiple catalytic functions of C_{50} carotenoid cyclases. *J. Bacteriol.* **192**, 5688–5699, https://doi.org/10.1128/JB.00724-10 (2010).
11. Krubasik, P., Kobayashi, M. & Sandmann, G. Expression and functional analysis of a gene cluster involved in the synthesis of decaprenoxanthin reveals the mechanisms for C_{50} carotenoid formation. *Eur. J. Biochem.* **268**, 3702–3708 (2001).
12. Tao, L., Yao, H. & Cheng, Q. Genes from a *Dietzia* sp. for synthesis of C_{40} and C_{50} beta-cyclic carotenoids. *Gene* **386**, 90–97, https://doi.org/10.1016/j.gene.2006.08.006 (2007).
13. Heider, S. A., Peters-Wendisch, P., Wendisch, V. F., Beekwilder, J. & Brautaset, T. Metabolic engineering for the microbial production of carotenoids and related products with a focus on the rare C_{50} carotenoids. *Appl. Microbiol. Biotechnol.* **98**, 4355–4368 (2014).
14. Abbes, M. *et al.* Biological properties of carotenoids extracted from *Halobacterium halobium* isolated from a Tunisian solar saltern. *BMC Complementary Altern. Med.* **13**, 255, https://doi.org/10.1186/1472-6882-13-255 (2013).

15. Mandelli, F., Miranda, V. S., Rodrigues, E. & Mercadante, A. Z. Identification of carotenoids with high antioxidant capacity produced by extremophile microorganisms. *World J. Microbiol. Biotechnol.* **28**, 1781–1790, https://doi.org/10.1007/s11274-011-0993-y (2012).
16. Yang, Y. *et al*. Complete Biosynthetic Pathway of the C_{50} Carotenoid Bacterioruberin from Lycopene in the Extremely Halophilic Archaeon *Haloarcula japonica*. *J. Bacteriol.* **197**, 1614–1623, https://doi.org/10.1128/JB.02523-14 (2015).
17. Furubayashi, M. *et al*. A highly selective biosynthetic pathway to non-natural C_{50} carotenoids assembled from moderately selective enzymes. *Nat. Commun.* **6**, 7534, https://doi.org/10.1038/ncomms8534 (2015).
18. Salis, H. M., Mirsky, E. A. & Voigt, C. A. Automated design of synthetic ribosome binding sites to control protein expression. *Nat. Biotechnol.* **27**, 946–950, https://doi.org/10.1038/nbt.1568 (2009).
19. Espah Borujeni, A., Channarasappa, A. S. & Salis, H. M. Translation rate is controlled by coupled trade-offs between site accessibility, selective RNA unfolding and sliding at upstream standby sites. *Nucleic Acids Res.* **42**, 2646–2659, https://doi.org/10.1093/nar/gkt1139 (2014).
20. Tian, T. & Salis, H. M. A predictive biophysical model of translational coupling to coordinate and control protein expression in bacterial operons. *Nucleic Acids Res.* **43**, 7137–7151, https://doi.org/10.1093/nar/gkv635 (2015).
21. Furubayashi, M. *et al*. A High-Throughput Colorimetric Screening Assay for Terpene Synthase Activity Based on Substrate Consumption. *PLoS ONE* **9**, e93317, https://doi.org/10.1371/journal.pone.0093317 (2014).
22. Umeno, D., Tobias, A. V. & Arnold, F. H. Diversifying carotenoid biosynthetic pathways by directed evolution. *Microbiol. Mol. Biol. Rev.* **69**, 51, https://doi.org/10.1128/MMBR.69.1.51-78.2005 (2005).
23. Lee, P. C., Momen, A. Z., Mijts, B. N. & Schmidt-Dannert, C. Biosynthesis of structurally novel carotenoids in *Escherichia coli*. *Chem. Biol.* **10**, 453–462 (2003).
24. Mijts, B. N., Lee, P. C. & Schmidt-Dannert, C. Identification of a carotenoid oxygenase synthesizing acyclic xanthophylls: Combinatorial biosynthesis and directed evolution. *Chem. Biol.* **12**, 453–460, https://doi.org/10.1016/j.chembiol.2005.02.010 (2005).
25. Kim, S. H., Kim, M. S., Lee, B. Y. & Lee, P. C. Generation of structurally novel short carotenoids and study of their biological activity. *Sci. Rep.* **6**, 21987, https://doi.org/10.1038/Srep21987 (2016).
26. Cunningham, F. X. Jr. & Gantt, E. One ring or two? Determination of ring number in carotenoids by lycopene epsilon-cyclases. *Proc. Natl. Acad. Sci. USA* **98**, 2905–2910, https://doi.org/10.1073/pnas.051618398 (2001).
27. Harrison, E. H. & Quadro, L. Apocarotenoids: Emerging Roles in Mammals. *Annu. Rev. Nutr.* **38**, 153–172, https://doi.org/10.1146/annurev-nutr-082117-051841 (2018).

Acknowledgements

This work was supported by Grants-in-Aid for Scientific Research from the Ministry of Education, Culture, Sports, Science and Technology [JSPS KAKENHI Grants 15H04189, 15K14228, and 16H06450], the Hamaguchi Foundation for the Advancement of Biochemistry, the Futaba Electronics Memorial Foundation, and the Shorai Foundation for Science and Technology. L.L. is supported by a JSPS fellowship for young scientists [JSPS KAKENHI Grant 15J07486].

Author Contributions

S.W., L.L., M.F. and D.U. conceived and designed the study. S.W. and L.L. performed experiments. M.F., L.L. and D.U. analyzed the results. T.M. performed NMR and MS/MS analysis. S.K.N., K.S. and D.U. supervised the study. M.F., L.L. and D.U. wrote the paper.

Additional Information

Supplementary information accompanies this paper at https://doi.org/10.1038/s41598-019-39289-w.

Competing Interests: The authors declare no competing interests.

Publisher's note: Springer Nature remains neutral with regard to jurisdictional claims in published maps and institutional affiliations.